APPLIED ORGANOMETALLIC CHEMISTRY
Appl. Organometal. Chem. 2001; **15**: 777–793
DOI: 10.1002/aoc.242

Precursor-derived Si–(B–)C–N ceramics: thermolysis, amorphous state and crystallization†

Joachim Bill,[1]* Thomas W. Kamphowe,[1] Anita Müller,[1] Thomas Wichmann,[1] Achim Zern,[1] Artur Jalowieki,[1] Joachim Mayer,[1] Markus Weinmann,[1] Jörg Schuhmacher,[2] Klaus Müller,[2] Jianqiang Peng,[1] Hans Jürgen Seifert[1] and Fritz Aldinger[1]

[1]Max-Planck-Institut für Metallforschung und Institut für Nichtmetallische Anorganische Materialien, Universität Stuttgart, Pulvermetallurgisches Laboratorium, Heisenbergstrasse 5, 70569 Stuttgart, Germany
[2]Institut für Physikalische Chemie, Universität Stuttgart, Pfaffenwaldring 55, 70569 Stuttgart, Germany

The preparation of silicon nitride- and carbide-based ceramics by solid-state thermolysis of polysilazanes and polysilylcarbodiimides is described. Results on the ceramization of the preceramic compounds and the architecture of the corresponding amorphous states obtained by spectroscopic means and by X-ray and neutron scattering are reviewed. Fundamental correlations between the composition and structure of the preceramic compounds and the architecture of the amorphous state are revealed. Furthermore, the crystallization behavior of the amorphous precursor-derived Si–C–N ceramics is treated. Moreover, the influence of boron on the thermal stability of the amorphous state is described. The high-temperature behavior of these Si–B–C–N solids can be correlated with their phase composition. Ceramic materials with compositions located close to the three-phase equilibrium SiC + BN + C exhibit a high temperature stability up to 2000 °C. This effect is accompanied by the formation of a metastable solid consisting of Si_3N_4 and SiC nanocrystals that are embedded in a turbostratic B–C–N matrix phase. Based on thermodynamic considerations, a model for the high-temperature stability effect is proposed. Copyright © 2001 John Wiley & Sons, Ltd.

Keywords: poly(boro)silazanes; Si–(B–)C–N ceramics; structural investigations

Received 4 April 2000; accepted 9 October 2000

1 INTRODUCTION

On the basis of their high strength and toughness, as well as on their thermal shock, corrosion and creep resistance, silicon nitride- and carbide-based ceramics provide a unique combination of properties with respect to high-temperature applications, e.g. in engines and turbines. In addition, these materials serve as cutting tools owing to their high hardness.

To date, powder technology represents the most common process for the preparation of silicon nitride ceramics, as well as of silicon nitride/carbide composites.[1–3] Owing to the low atomic mobilities, which trace back to the covalent nature of these ceramics, auxiliary materials like yttria, alumina or magnesia have to be added for the densification of the corresponding ceramic powders. As a result, this process yields polycrystalline microstructures that contain oxide-based grain-boundary phases.

In contrast to the evolution of microstructures from ceramic powders, the architecture from molecular units represents a means for the design of ceramic microstructures on an atomic scale, and thus for increasing the ability to control the structure and hence the properties of ceramic solids. In this connection, molecular design enabled

* Correspondence to: J. Bill, Max-Planck-Institut für Metallforschung und Institut für Nichtmetallische Anorganische Materialien, Universität Stuttgart, Pulvermetallurgisches Laboratorium, Heisenbergstrasse 5, 70569 Stuttgart, Germany.
Email: bill@aldix.mpi-stuttgart.mpg.de
† Dedicated to Professor Wolfgang Laqua on the occasion of his 65th birthday.
Contract/grant sponsor: Deutsche Forschungsgemeinschaft.
Contract/grant sponsor: Japan Science and Technology Corporation (JST).

by solid-state thermolysis of preceramic compounds allows the preparation of ceramic solids without any additives and thus provides a means to exploit the properties of the phase-pure materials.[4–11] This route involves the thermal transformation of precursors into metastable amorphous ceramic materials *via* the condensed state. Further heat treatment then induces the transformation into crystalline phases.

It is the purpose of this paper to combine results of different previous studies and recent unpublished data in order to present a comprehensive description of the structure formation during ceramization of preceramic Si–(B–)C–N polymers and the crystallization of the corresponding amorphous ceramic materials. Within Section 2 the polysilazane and polysilylcarbodiimide polymer systems are presented. Section 3 reviews prior published findings that concern the correlation of the molecular structure and composition of Si–C–N precursors with the structure of the corresponding amorphous ceramics. In this connection, the thermally induced ceramization of these precursors, as well as the architecture of the amorphous ceramic solids, is described. Furthermore, these observations are related to energetic considerations by the CALPHAD (CALculation of PHAse Diagrams[12]) approach in order to provide a quantitative base for the description of the thermal behavior of these material systems.

Section 4 introduces the basic features of the crystallization behavior of the amorphous ternary and quaternary Si–(B–)C–N ceramics. In addition, new results obtained by the transmission electron microscopy (TEM) characterization of the grain-boundary phases within nanocrystalline Si–B–C–N solids are introduced. Furthermore, these results are correlated with the high-temperature stability of these solids and discussed in combination with the phase equilibria of the quaternary system Si–B–C–N.

2 POLYMER SYSTEMS

The preceramic polymers employed for the preparation of ternary Si–C–N ceramics in this study are shown in Fig. 1.[13] The polymers consist of a silicon-containing backbone and side groups connected to the silicon atoms. The second unit constituting the backbone is —NH— groups in the case of polysilazanes[5–7,9,14–17] and carbodiimide groups in the case of polysilylcarbodiimides.[18–22] These polymers are obtained by the condensation reaction of organochlorosilanes with ammonia and cyanamide respectively. In contrast to reactions involving the formation of the solid by-products ammonium chloride and pyridinium hydrochloride py·HCl, polysilylcarbodiimides can also be obtained *via* the reaction of organochlorosilanes with bis(trimethylsilyl)carbodiimide, yielding trimethylchlorosilane as a by-product, which can be easily removed by distillation.[21,23,24]

As can be seen from Fig. 1, the molecular structure and the side groups that are connected to silicon vary depending on the organosilane initially used. According to these routes, precursors like polymethylvinylsilazane (PMVS),[6,25] polyhydridomethylsilazane (PHMS)[26] as well as the corresponding polysilylcarbodiimides PMVC[18] and PHMC[27] have been synthesized.

Besides Si–C–N precursors, preceramic compounds for Si–B–C–N ceramics have gained significance because of the outstanding thermal stability of the resulting quaternary ceramics. Basically, the synthesis of these compounds can be carried out in two ways:

- chemical modification of silicon-containing polymers or oligomers with boron-containing compounds (polymer route);
- synthesis of polymers from boron-containing monomer units (monomer route).

Initial work was done by Takamizawa *et al.*, who synthesized Si–B–C–N precursors from mixtures of organopolysilane and organoborazine compounds suitable for the preparation of Si–B–C–N ceramic fibers.[27,28] In addition, boranes[29–32] have been applied for the modification of silazanes. Furthermore, borazine-based Si–B–C–N precursors have been synthesized.[33–36] In this connection, Sneddon and coworkers succeeded in the modification of polyhydridopolysilazane with borazine *via* the polymer route:[34–36]

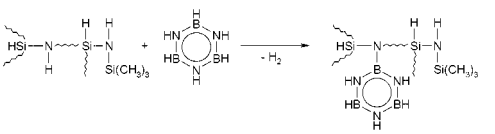

[1]

Pioneering work with respect to the monomer route was done by Jansen and coworkers,[37–40] who synthesized the single-source precursor (*t*richlorosilyl*a*mino)-*d*ichloro*b*orane) (TADB) Cl_3Si—NH—BCl_2, which can be transformed into Si–B–C–N preceramic polymers by the subsequent polycondensation reaction with aliphatic amines.

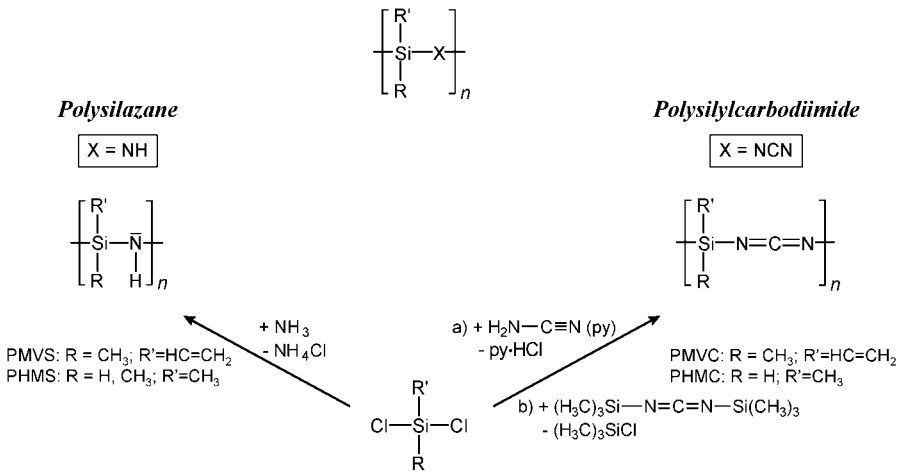

Figure 1 Synthesis of polysilazane and polysilylcarbodiimide precursors.

A completely novel approach according to the monomer route was demonstrated by Jones and Myers[41] and Riedel and coworkers,[42–45] who employed monomers obtained by the hydroboration reaction of dichloromethylvinylsilane ($R = CH_3$) with Lewis base adducts $L{\cdot}BH_3$ (Fig. 2a) and chloroborane adducts respectively.

Polymer formation is achieved by subsequent ammonolysis.[46–49] Besides dichloromethylvinylsilane, dichlorovinylsilane[50] ($R = H$) has also been applied for polymer synthesis *via* this route.[51–53] As initially suggested by Matsumoto and Schwark,[54] this kind of polymer system can also be obtained from polyvinylsilazanes, like PMVS, PHVS or PNVS, and boranes *via* the polymer route (Fig. 2).[51–53]

This kind of synthesis strategy also serves for the preparation of boron-containing polysilylcarbodii-

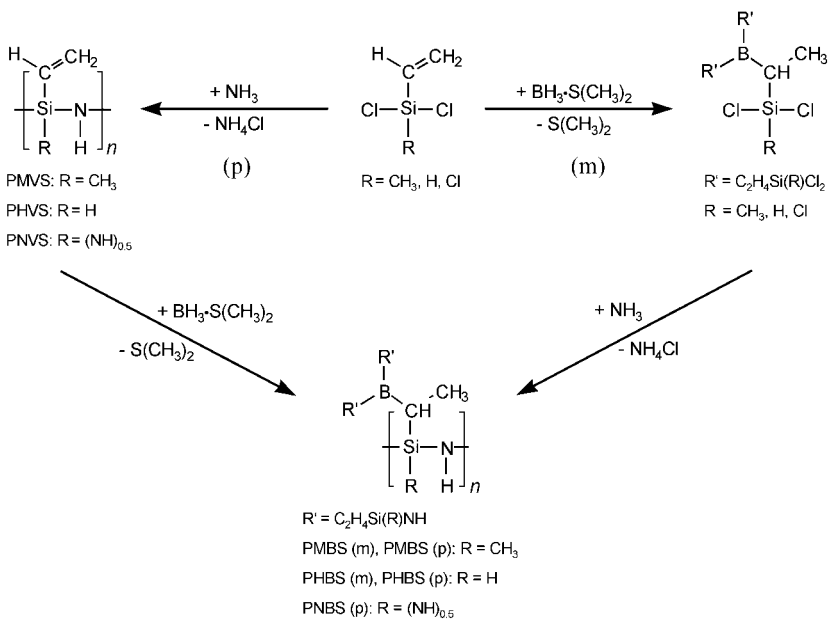

Figure 2 Synthesis of boron-containing polysilazanes *via* the monomer (m) and the polymer (p) route.

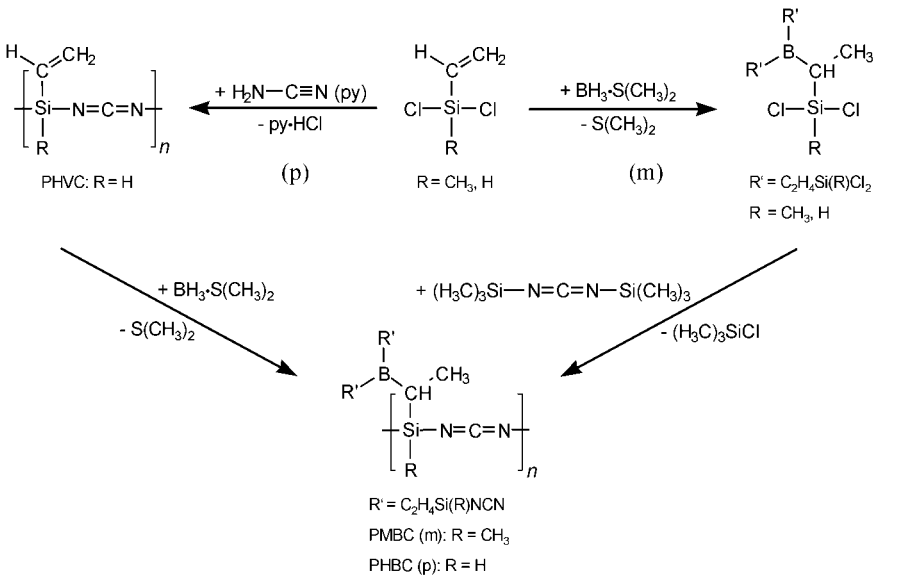

Figure 3 Synthesis of boron-containing polysilylcarbodiimides *via* the monomer (m) and the polymer (p) route.

mides (Fig. 3). On the one hand, polysilylcarbodiimides that contain vinyl groups can be reacted with dimethylsulfide borane *via* the polymer route[55–58] (Fig. 3). On the other hand, boron-containing monomers can be reacted with bis(trimethylsilyl)-carbodiimide (Fig. 3). Because of the pseudochalcogenic character of the carbodiimide group, this reaction can be considered to be a non-oxide sol–gel process for the preparation of Si–B–C–N precursors, which can be carried out with or without solvents (Fig. 3).[56–58]

Besides hydroboration reactions, hydrosilylation involving liquid mixtures of vinylsilazanes[50] and tris(hydridosilylethyl)boranes[59] can also be used in the formation of preceramic networks for the preparation of quaternary Si–B–C–N ceramics (Eqn [2]).[60–62]

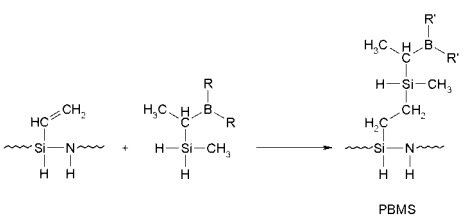

[2]

The thermally induced hydrosilylation reaction at 180 °C can be carried out without solvents and leads to a solidification yielding a glass-like solid without the formation of by-products.* As a result, this reaction can be applied as a matrix source for fiber-reinforced ceramic matrix composites by a resin transfer molding (RTM) process. According to this process, fabrics made of carbon fibers are infiltrated with the reaction mixture, which is then transformed into a solid polymer matrix at 180 °C according to Eqn [2]. Subsequent thermolysis transforms the polymer matrix into an Si–B–C–N ceramic matrix, yielding a carbon-fiber-reinforced Si–B–C–N composite material.[60–62]

3 CERAMIZATION AND THE AMORPHOUS STATE

The preceramic compounds PHMS, PMVS,

* H magic angle spinning (MAS) NMR: δ −0.1 (SiCH_3), 0.8 (N*H*, var. C*H*), 3.6 (C_3Si*H*), 4.5 (N_2Si*H*). ^{13}C cross-polarization (CP)-MAS NMR: δ −6.5 (SiCH_3), 13.5 (SiCH_2, $CHCH_3$). ^{29}Si CP-MAS NMR: δ −31.4 ($H_2SiC_2(sp^3)$), −18.0 ($HSiN_2C(sp^3)$), −11.5 ($HSiC_3(sp^3)$).

Solid-state NMR experiments were performed on a Bruker CXP 300 or a Bruker MSL 300 spectrometer operating at a static field of 7.05 T (^{1}H frequency: 300.13 MHz) using a 4 mm MAS probe. ^{29}Si and ^{13}C spectra were recorded at 59.60 and 75.47 MHz using the CP technique in which a spin lock field of 62.5 kHz and a contact time of 3 ms were applied. Typical recycle delays were 6 to 8 s. All spectra were acquired using the MAS technique with a sample rotation frequency of 5 kHz. ^{29}Si and ^{13}C chemical shifts were determined relative to external standard Q_8M_8, the trimethylsilylester of octameric silicate, and adamantane respectively. These values were then expressed relative to the reference compound tetramethylsilane (0 ppm).

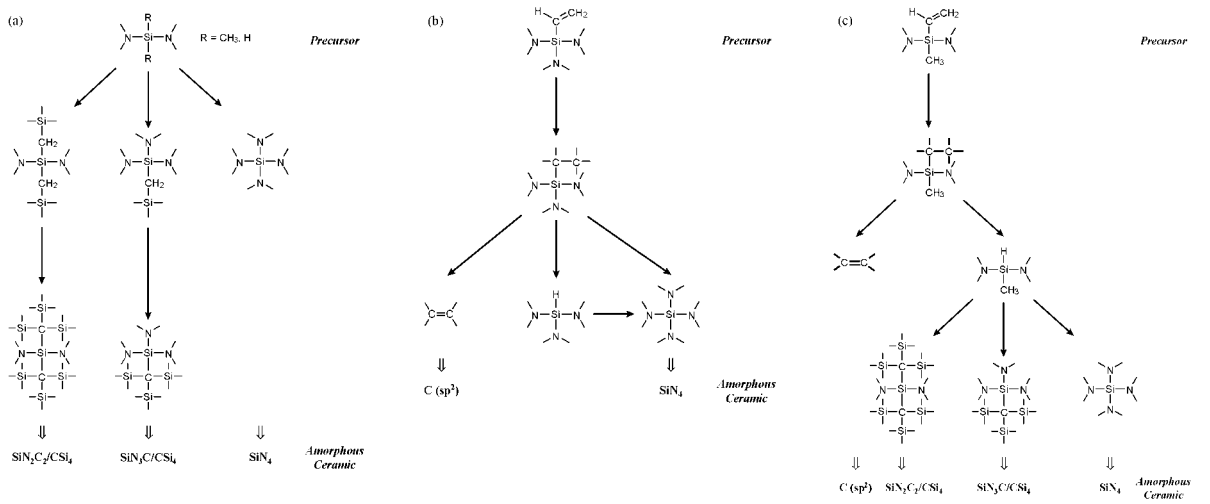

Figure 4 Evolution of structural units during the conversion of the polysilazanes (a) PHMS, (b) PNVS and (c) PMVS into amorphous Si–C–N ceramics.

PHMC, PMVC (Fig. 1) and PNVS[14] (Fig. 2) are transformed into amorphous Si–C–N ceramic solids by thermolysis at temperatures around 1050 °C, which is accompanied by the formation of volatile hydrogen-containing by-products. The evolution of the structural units of the polysilazane precursors into amorphous Si–C–N ceramic solids up to 1050 °C, as investigated by solid-state NMR, IR and mass spectroscopy, is shown in Fig. 4.[13,17]

The investigation of the ceramization by ^{13}C and ^{29}Si solid-state NMR, IR and mass spectroscopy reveals, in the case of the polymer PHMS, cross-linking reactions that involve Si—CH_3 and Si—H units accompanied by the evolution of methane and hydrogen:[17]

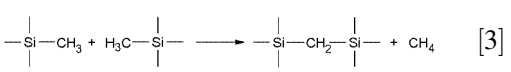
[3]

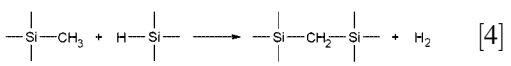
[4]

These polycondensation reactions occur at temperatures around 500 °C, and most likely follow radical mechanisms initiated by a homolytic cleavage of Si—C bonds.[63–67] If the temperature is raised to 1050 °C these reactions proceed further, finally resulting in the formation of tetrahedral CSi_4 structural units:


[5]

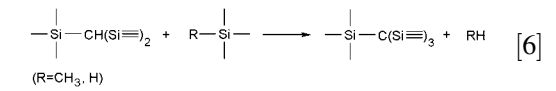
[6]

At temperatures above 500 °C, Si—N bonds are formed *via* condensation reactions involving N—H units:

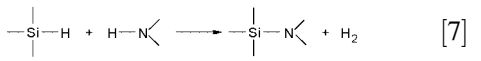
[7]

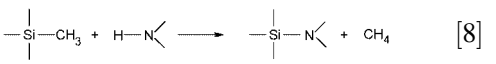
[8]

Owing to these reactions, the amount of SiN_3C and SiN_4 sites increases continuously at the expense of SiN_2CH and SiN_2C_2 units. Finally, an amorphous covalent solid is obtained at 1050 °C that consists of SiN_4, SiN_3C, SiN_2C_2 and CSi_4 units. In addition, the structural units of sp^2-hybridized carbon are present in the amorphous state due to the thermal decomposition of the gaseous by-product methane above 500 °C:[13]

$$CH_4 \rightarrow C_{sp^2} + 2H_2 \qquad [9]$$

Thermal treatment of the polymer PNVS up to 300 °C induces cross-linking by polymerization of the vinyl groups (Fig. 4b).[13] If the temperature is raised further the formation of Si—H and sp^2-

hybridized carbon units occurs:

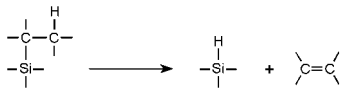

[10]

Investigations on model compounds suggest that this reaction is initiated by the homolytic cleavage of Si—C bonds followed by the β-elimination of a hydrogen radical.[63] Subsequent reaction of the Si—H units according to Eqn [7] around 500 °C leads to Si—N bonds. As a result, Si—C bonds present in the preceramic polymer are quantitatively cleaved along with formation of Si—N bonds, yielding an amorphous ceramic solid at 1050 °C that is built up by SiN_4 groups. Moreover, ammonia can be detected by mass spectroscopy between 200 and 500 °C,[13] suggesting a transamination reaction[64,65] that affects =N—H silazane groups and yields NSi_3 units, leading to a reduction of the nitrogen content present in the solid phase:

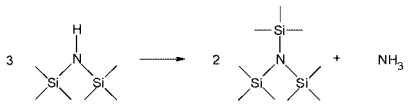

[11]

Besides these structural units of silicon nitride, sp^2-hybridized carbon units formed according to Eqn [10] are present within the amorphous ceramic state. Moreover, the thermal degradation of the hydrocarbon chains of the cross-linked polymer (Fig. 4b) leads to the evolution of methane, which subsequently contributes to the content of solid carbon, as described in Eqn [9].[13]

The preceramic compound PMVS contains both Si—CH_3 and Si—CH=CH_2 units (Fig. 2) and can be considered a hybrid of the polymers PHMS and PNVS. Therefore, ceramization mechanisms described above for these two polymers are observed. As can be seen from Fig. 4c, the reactions mentioned in Eqns [3]–[10] occur during ceramization, finally resulting in an amorphous ceramic solid made of SiN_xC_y ($x = 2$–4, $x + y = 4$) and CSi_4 sites, as well as of sp^2-hybridized carbon units.[13]

The ceramization of the precursors PHMC and PMVC into amorphous ceramic solids involves the quantitative thermal degradation of the carbodiimide groups, as revealed by solid-state NMR and IR spectroscopy.[13] This degradation is accompanied by the formation of the structural units of silicon nitride as well as by the evolution of $(CN)_2$ and CH_3CN, suggesting the following transformation reactions:

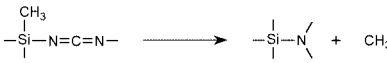

[12]

[13]

As a result, the investigation by spectroscopic means of the amorphous ceramics obtained reveals the presence of SiN_4 sites and sp^2-hybridized carbon units exclusively.[13] These carbon units trace back to the thermal decomposition of the gaseous by-products mentioned in Eqns [12] and [13] into the elements. Moreover, the transformation reaction [9] of methane that evolves during thermolysis and the β elimination (Eqn [10]) in the case of PMVC (Fig. 1) represent further pathways for the incorporation of solid carbon.[13]

In the case of the model systems described above, the composition of the initially used precursors strongly determines the structure and composition of the corresponding amorphous ceramics (Figs 5 and 6). Polymer compositions within the subtetrahedron Si_3N_4–C–H–N behind the plane Si_3N_4–C–H of the Si–C–H–N concentration tetrahedron (PNVS, PMVC, PHMC) yield ceramics with compositions located close to the tie line silicon nitride–carbon. In the case of polymer compositions found in front of this separating plane inside the subtetrahedron Si_3N_4–SiC–C–H (PHMS,

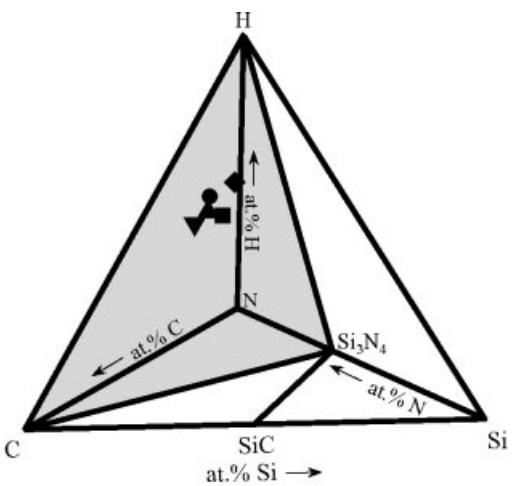

Figure 5 Si–H–C–N concentration tetrahedron. The compositions of the precursors PNVS (■), PMVC (▼) and PHMC (▲) behind, and of PHMS (◆) and PMVS (●) in front of the plane Si_3N_4–C–H are inserted.

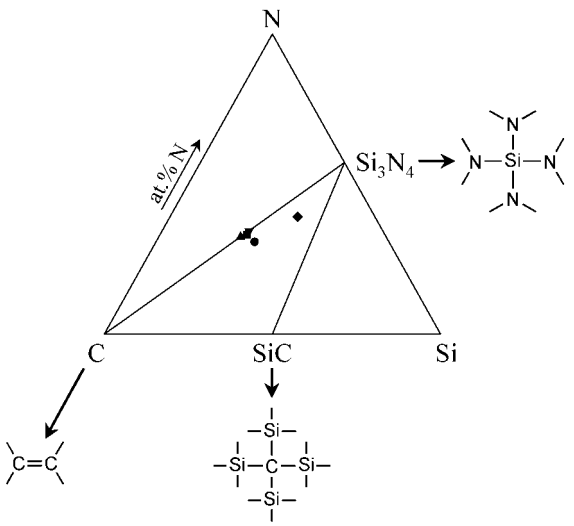

Figure 6 Si–C–N phase diagram[12] valid up to 1484 °C. The compositions of the amorphous Si–C–N ceramics derived from the precursors PHMS (◆), PMVS (●), PHMC (▲), PNVS (■) and PMVC (▼) are inserted. Furthermore, the structural units of silicon nitride, carbide and carbon are indicated.

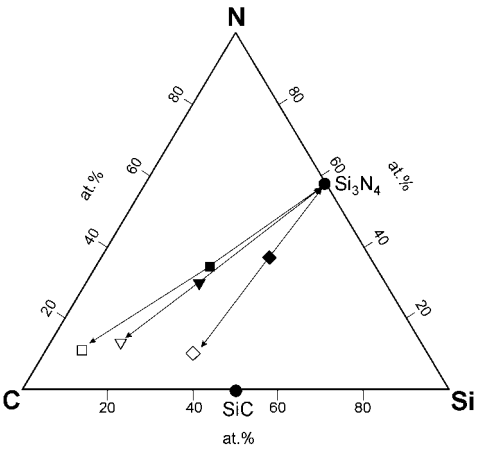

Figure 8 Si–C–N concentration triangle. The compositions of the PNVS- (■), PHMS-(◆) and PMVC-derived (▼) ceramics as well as of the corresponding matrix phases (empty symbols) obtained by subtraction of the segregated silicon nitride phase amount are inserted.

PMVS), ceramic compositions within the tie triangle Si_3N_4–SiC–C are obtained.

These results are in accordance with thermodynamic calculations, indicating that the transformation of the precursors considered is influenced strongly by the minimization of the Gibbs energy of the system[13] (also, see Ref. 12).

Comparison with the above-mentioned structural investigations shows a correlation of the short-range order with the composition of the X-ray-amorphous solids. The compositions of the PNVS-, PHMC-, and PMVC-derived amorphous ceramics are located close to the tie line Si_3N_4–C. In these cases, the amorphous ceramic states are built up by SiN_4 sites and sp^2-hybridized carbon units.[13,17] The PHMS- and PMVS-derived materials exhibit compositions within the three-phase equilibrium field Si_3N_4–SiC–C and consist of silicon carbide units, CSi_4, as well as mixed tetrahedrons SiN_xC_y ($x = 2$,

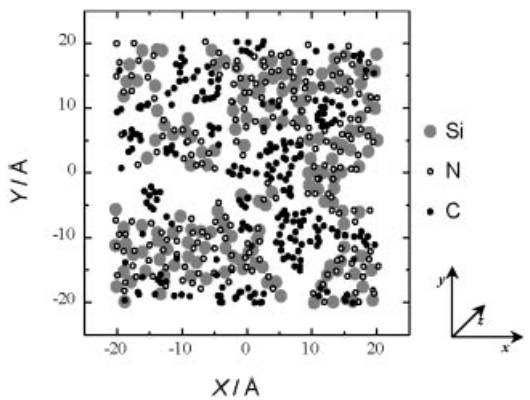

Figure 7 Reverse Monte Carlo model of the amorphous ceramic solid derived from the polysilylcarbodiimide PHMC. The model shows an orthogonal projection of the silicon, nitrogen and carbon atoms within the range $-15 < Z < -10$ Å.

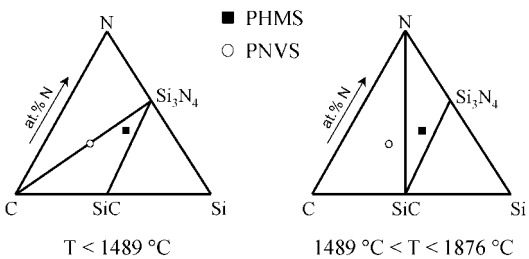

Figure 9 Phase equilibria for the ternary system Si–C–N below and above 1484 °C. The compositions of the PHMS- and PNVS-derived ceramics are inserted. The total pressure is considered to be 1 bar.

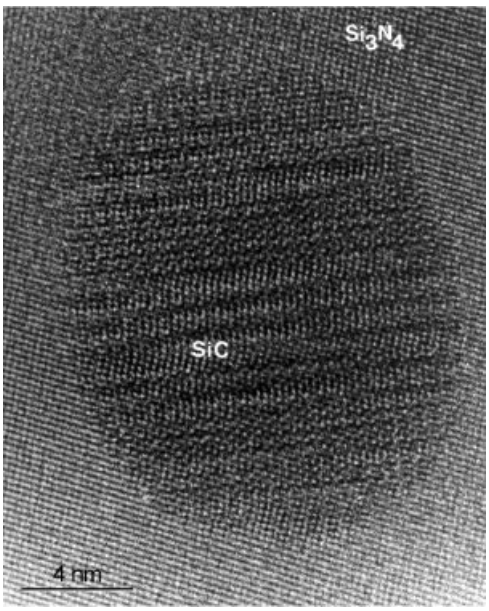

Figure 10 HRTEM image showing a SiC inclusion within a matrix made of Si_3N_4. The material is derived from the polysilazane PHMS and subsequently annealed for 50 h at 1800 °C in a nitrogen atmosphere.

3; $x + y = 4$) and SiN_4 and sp^2-hybridized carbon sites. As a consequence, the structural units of the thermodynamically stable phases are already preformed within the amorphous ceramics. Moreover, these observations are also valid for the medium-range structure. In Fig. 7 a reverse Monte Carlo model of the PHMC-derived amorphous solid based on X-ray and neutron wide-angle scattering data is shown.[68]

In accordance with the location of the composition close to the tie line Si_3N_4–C within the phase diagram, the material consists of two separate phases, silicon nitride and carbon, with sizes in the region of 10 Å. Residual amounts of nitrogen in the carbon phase cannot be detected.

Recently, a phase separation was also observed for the amorphous ceramic solids derived from the precursors PHMS, PNVS and PMVS by X-ray and neutron small-angle scattering.[13] Owing to these investigations, the as-received ceramics contain an amorphous silicon nitride separation phase that exhibits a Guinier radius in the range between 5 and 10 nm. The composition of the remaining amorphous matrix after subtraction of the volume fraction of the separated silicon nitride phase is shown in Fig. 8. As can be seen from this diagram, the amorphous ceramic solids derived from the precursors PNVS and PMVC contain a carbon-enriched matrix phase, whereas the matrix composition of the PHMS-derived material is shifted to the SiC region of the concentration triangle.

4 CRYSTALLIZATION BEHAVIOR

Further heat treatment of the amorphous ternary ceramic solids leads to the formation of the thermodynamically stable phases. The corresponding phase equilibria can be seen in Fig. 9. As can be seen from these diagrams silicon, nitride is stable in the presence of carbon below 1484 °C. Above this temperature the silicon nitride reacts with carbon to give silicon carbide with loss of nitrogen:

$$Si_3N_4 + 3C \rightarrow 3SiC + 2N_2 \qquad [14]$$

The PNVS-derived material remains X-ray-amorphous after annealing at 1450 °C for 50 h in a nitrogen atmosphere, indicating that grain growth and crystallization of the amorphous silicon nitride phase present within the as-received material (see Section 3) are retarded by the surrounding carbon-enriched matrix phase.[17] TEM investigations reveal that crystallization is induced at 1500 °C and accompanied by the loss of the nitrogen, yielding a silicon carbide/carbon composite ceramic.

In the case of the ceramic solid obtained from the polysilazane PHMS, at first microcrystalline areas

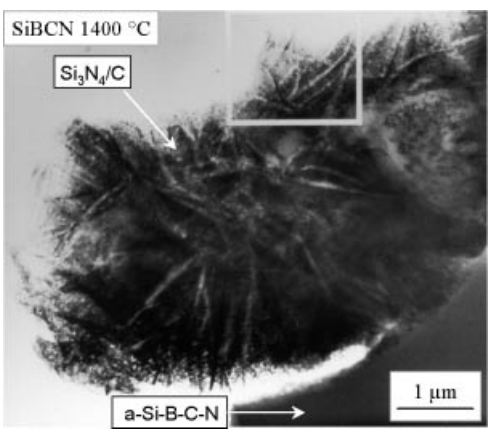

Figure 11 Bright-field image of the PHMS(B)-derived ceramic doped with 1.8 at.% boron after annealing at 1400 °C for 50 h in a nitrogen atmosphere. The area that corresponds to the elemental distribution images in Fig. 20 is indicated.

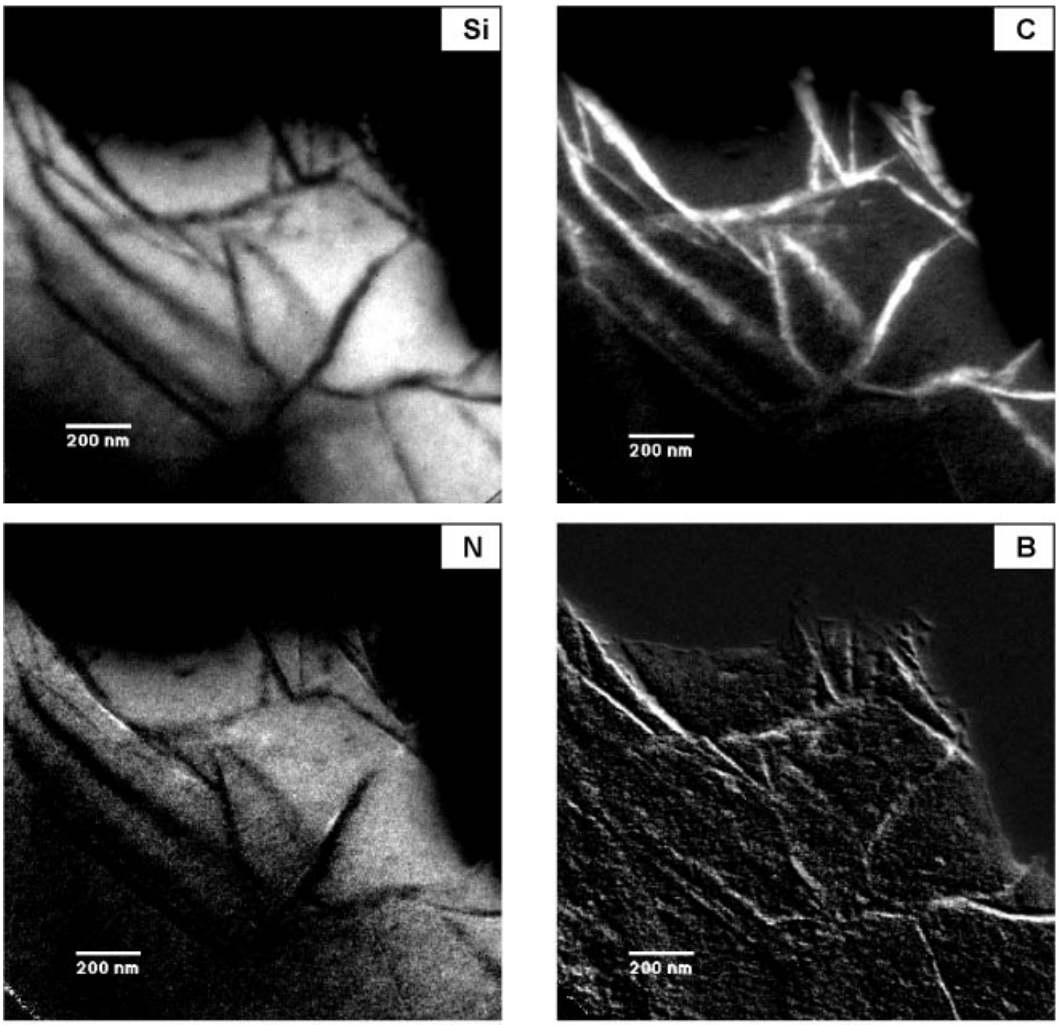

Figure 12 Elemental distribution image for silicon, carbon, nitrogen and boron of the PHMS-derived ceramic doped with 1.8 at.% boron after annealing at 1400 °C for 50 h in a nitrogen atmosphere.

made of silicon nitride can be detected, in addition to carbon-enriched areas after annealing at 1350 °C. From 1500 °C on, the thermal degradation of the material leads to the evolution of nitrogen and crystalline SiC (Eqn [14]), finally resulting in a crystalline silicon nitride/carbide composite (Fig. 10). As can be seen from the high-resolution TEM (HRTEM) image in Fig. 10, completely 'clean' grain boundaries between the silicon nitride and carbide crystals are formed.

Additional phases can be introduced by the incorporation of further elements that lead to segregations at the grain boundaries during the *in situ* crystallization of the material. Doping of the PHMS-derived ceramic with boron can be achieved by the chemical modification of the initially applied polysilazane PHMS with tris(dimethylamino)borane[69] (PHMS(B)). Thermolysis yields an amorphous ceramic solid with a boron content of 1.8 at.%. If this material is annealed at 1400 °C, the relative amount of crystalline silicon nitride is reduced significantly compared with the corresponding ternary Si–C–N material, indicating a stabilization of the amorphous state by the incorporation of boron. Recent TEM results reveal that these crystalline areas within the amorphous

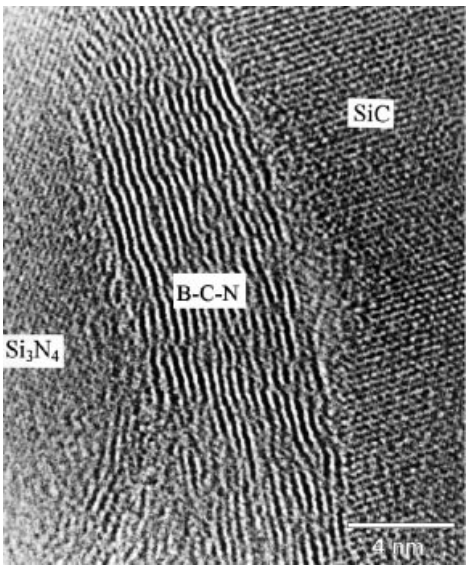

Figure 13 HRTEM image of the PHMS(B)-derived ceramic doped with 1.8 at.% boron after annealing at 1800 °C for 50 h in a nitrogen atmosphere.[71] Reprinted from *Composites Part A*, **27A**, A. Jalowiecki, J. Bill, F. Aldinger, J. Mayer, 'Interface Characterization of Nanosized B-Doped Si_3N_4/SiC Ceramics', page 721, Copyright (1996), with permission from Elsevier Science.

Si–B–C–N phase (a-Si–B–C–N) are combined with carbon-containing segregations (Fig. 11).*

Owing to this phase separation, boron is enriched within the carbon-based phase along the grain boundaries of the silicon nitride crystals, as can be seen from the elemental distribution images in Fig. 12.

Further heat treatment of the material at 1800 °C leads to the formation of crystalline silicon nitride and silicon carbide, which exhibit a grain size in the region of 50 nm. Compared with the corresponding boron-free material, the crystal size is significantly reduced. The further characterization by elemental distribution images and HRTEM reveals the presence of a boron-, carbon- and nitrogen-containing grain-boundary phase that exhibits a turbostratic character (Fig. 13).[71]

Obviously, the segregation of this turbostratic phase at the grain boundaries retards crystal growth. In addition, the presence of carbon within the grain boundaries reveals the metastable character of the B–C–N phase. Calculated phase equilibria in the quaternary Si–B–C–N system at constant temperatures and boron contents are shown in Fig. 14. For further details on interpretation of such diagrams see Refs 12 and 70. As can be seen from Fig. 14a, the equilibrium phases at 1800 °C are $Gas(N_2) + Si_3N_4 + SiC + BN$.

As a result, a quantitative degradation of carbon according to Eqn [14] is not observed, suggesting that the presence of boron and nitrogen within the grain-boundary phase leads to a decrease of the activity and thus to an increase of the temperature of reaction [14] (also, see Ref 12.).

The calculated phase equilibria in Fig. 14 also contain the compositions† of the amorphous ceramics obtained by the thermolysis of precursors described in Section 3. Moreover, the ceramic compositions obtained from the polymers B-HPZ 3 and B-HPZ 4 synthesized and reported by Sneddon and coworkers (see Eqn [1], Section 2)[34,35] are inserted. As can be seen from the diagrams valid at 1400 °C, all compositions considered are located within the four-phase equilibrium system $Si_3N_4 + SiC + C + BN$. The compositions derived from the precursors PBMS, PMBS and PHBS are found within the silicon-carbide-rich part close to the three-phase equilibrium field $SiC + C + BN$. Comparatively, the ceramic compositions obtained from B-HPZ 3, PMBC, PHBC, PHMS(b), PNBS and B-HPZ 4 are shifted to silicon-nitride-enriched areas.

A feature characteristic for the first-mentioned class of materials is the presence of silicon carbonitride units SiC_xN_y ($x = 1,\ 2;\ x + y = 4$) within the amorphous state.[72–74] Furthermore, these solids consist of CSi_4 units, as well as of sp^2-hybridized carbon and boron-containing units, which is demonstrated by means of the ^{29}Si, ^{13}C and ^{11}B solid-state NMR spectra obtained for the PMBS-derived ceramic (Fig. 15).

The comparison with the ^{29}Si NMR spectrum of

* For the TEM investigations PHMS(B)-derived Si-B-C-N ceramics were synthesized according to Ref. 70. PHBS-derived materials were obtained according to Ref. 51. They were subsequently annealed using a graphite furnace (heating rate $T < 1400$ °C: 10 °C min^{-1}; $T = 1400$–1800 °C: 2 °C min^{-1}) and a carbon crucible.

Electron-transparent specimens were obtained by mechanically sectioning the materials, polishing and dimpling 3 mm discs, followed by a final Ar^+ ion-beam thinning. The energy filtering TEM (EFTEM) investigations were performed on a Zeiss EM 912 Omega, which was operated at 120 kV and was equipped with an LaB_6 cathode. Electron spectroscopic imaging (ESI) image filter series were recorded on a GATAN 1024 × 1024 slow scan CCD camera using GATAN's Digital Micrograph software. The required image processing routines were written in the script language within Digital Micrograph and the quantitative analysis was performed using the GATAN EL/P programm package.

† Chemical analysis was performed using a combination of different analysis equipment (ELEMENTAR Vario EL, ELTRA CS 800 C/S Determinator, LECO TC-436 N/O Determinator) and by atom emission spectrometry (ISA JOBIN YVON JY70 Plus).

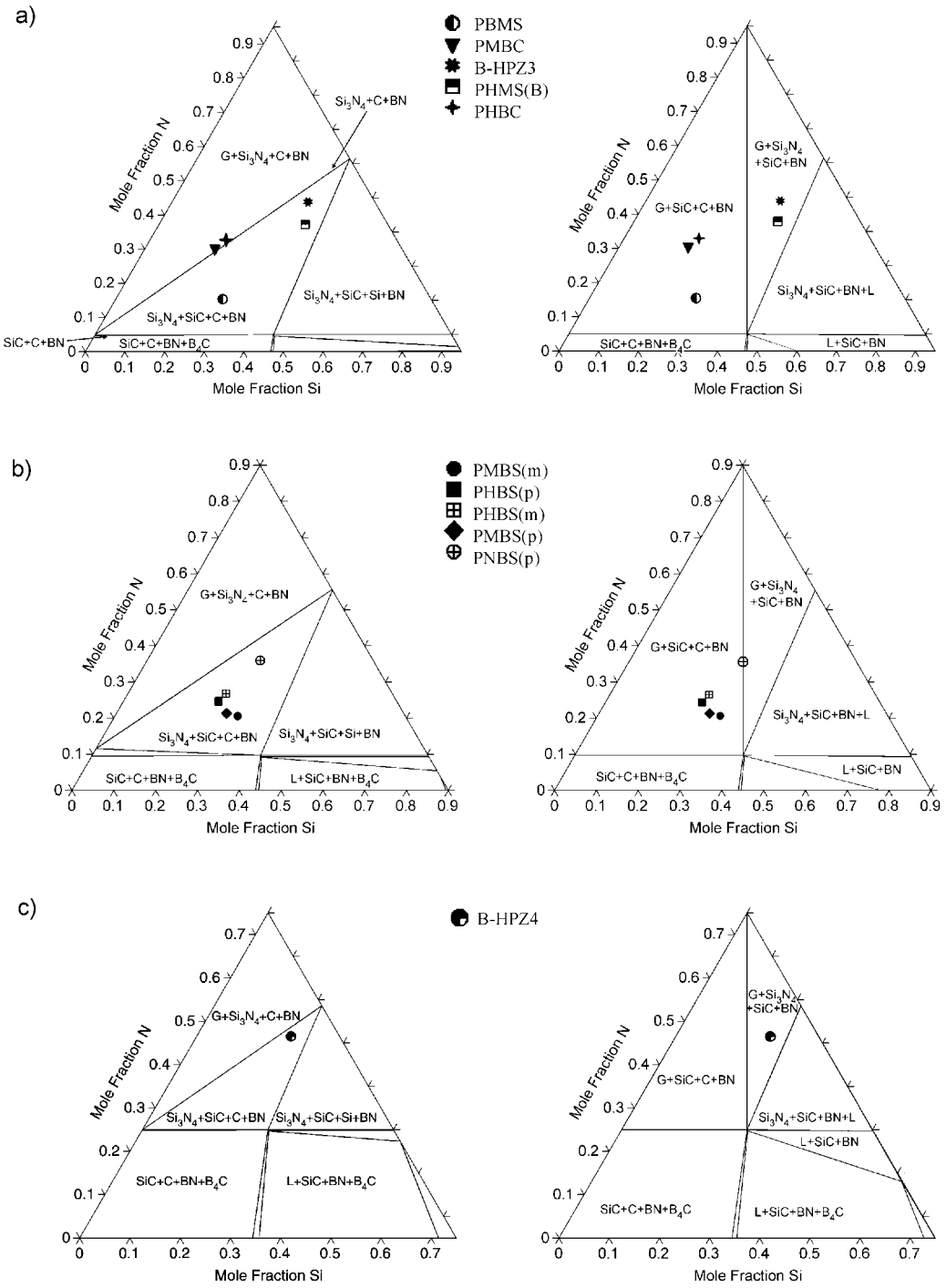

Figure 14 Calculated phase equilibria in the quaternary Si–B–C–N system at constant boron contents of (a) 5.0, (b) 9.7 and (c) 25.0 at.% at 1400 and 1800 °C at $p_{total} = 1$ bar. The compositions of the ceramics derived from the polymers PBMS, PMBC, PHMS(B), PHBC, PMBS ((m) and (p)), PHBS ((m) and (p)) and PNBS are inserted. The diagrams also contain the ceramic compositions that evolve from the polymers B-HPZ 3 and B-HPZ 4 as reported by Sneddon[3] and coworkers.[34,35].

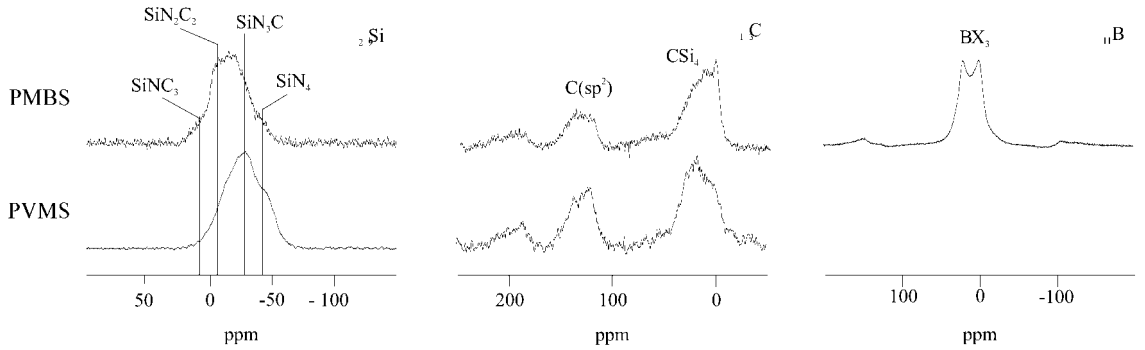

Figure 15 ^{29}Si, ^{13}C and ^{11}B solid-state NMR spectra of the amorphous PMBS-derived Si–B–C–N ceramic, as well as of the corresponding boron-free PMVS-derived Si–C–N solid.[72].

the corresponding boron-free ternary ceramic solid (Fig. 15) further suggests the formation of B—N bonds, because of the significant reduction of the relative amount of Si—N bonds and SiN_4 units if boron is incorporated into the amorphous state.

These results indicate that the short-range order within the amorphous state is influenced by the composition of the Si–B–C–N ceramics, in accordance with the results for the ternary solids described in Section 3. This observation is also supported by the short-range order of the PMBC-derived material attributed to the nitrogen-enriched

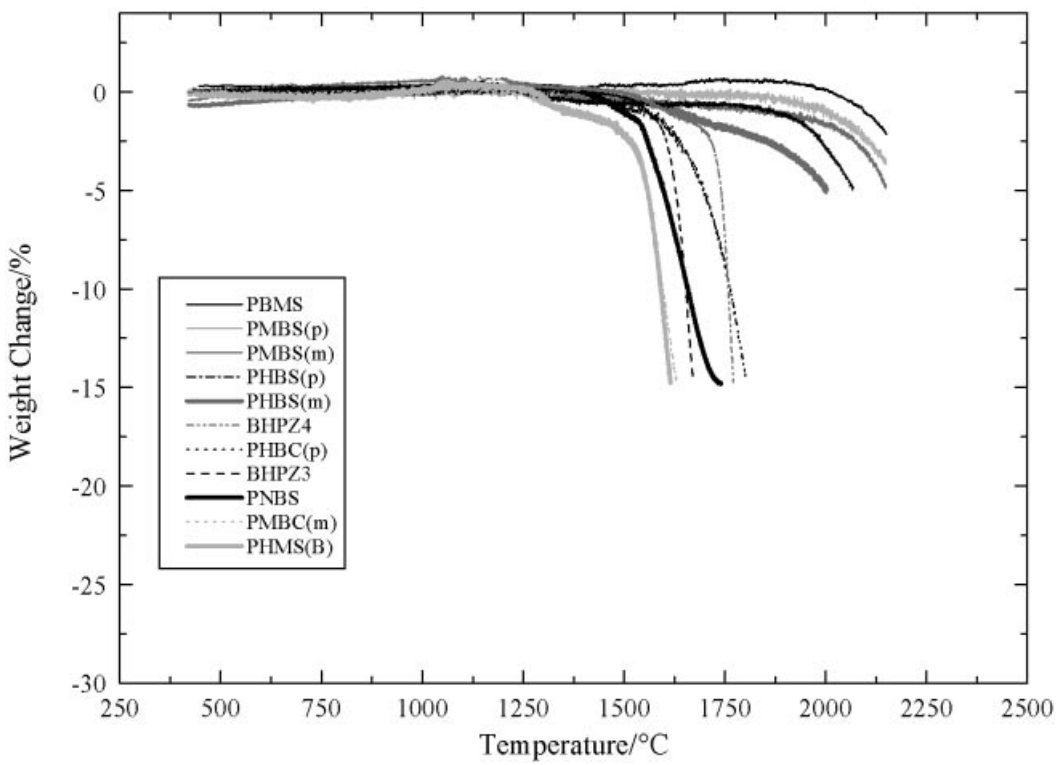

Figure 16 Thermal gravimetric analysis (argon atmosphere) of the Si–B–C–N ceramics described in Fig. 14.

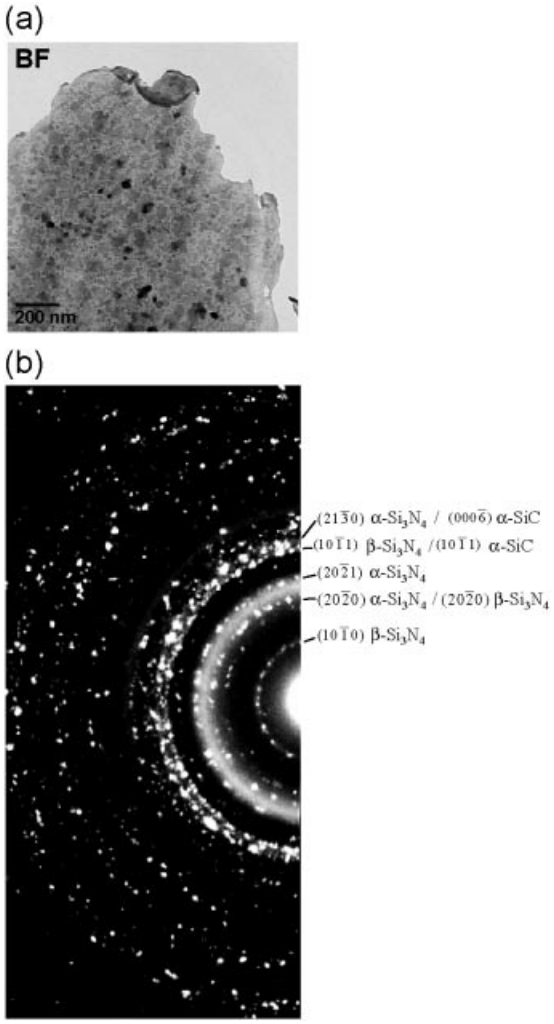

Figure 17 Bright-field image of PHBS(p)-derived ceramic after annealing at 1800 °C (5 h, argon) (a) and corresponding selected-area electron diffraction pattern (b).

ceramic solids mentioned above. In this material, which exhibits a composition close to the three-phase equilibrium field $Si_3N_4 + C + BN$ (Fig. 14a), the SiN_4 structural units of silicon nitride, as well as sp^2-hybridized units of boron nitride and carbon, are found by solid-state NMR spectroscopy.[74,75]

Furthermore, the composition and the architecture of the amorphous state strongly determine the high-temperature and crystallization behavior of the Si–B–C–N ceramics. Ceramic solids with a composition close to the three-phase equilibrium field $SiC + C + BN$ show an extraordinary high-temperature stability (Fig. 16).

By contrast with the remaining Si–B–C–N ceramics, the weight loss due to the evolution of nitrogen (Eqn [14]) is significantly reduced even at 2000 °C. Further investigations on the crystallization behavior reveal that amorphous solids like the PMBS-derived ceramic resist crystallization below 1700 °C.[48,49] Within the resulting crystalline areas, silicon nitride is detected experimentally, in addition to silicon carbide, whereas the phase equilibria shown in Fig. 14b indicate the instability of silicon nitride at this temperature (1800 °C).

A typical microstructure of this kind is shown in Fig. 17 by means of the TEM bright-field image observed for the PHBS(p)-derived ceramic after annealing at 1800 °C (5 h; argon); see previous footnote for TEM conditions. The material consists of nanocrystals with a size in the region of 50 nm embedded into an amorphous matrix phase. Electron (Fig. 17b) and X-ray diffraction reveal the presence of silicon nitride and silicon carbide. In Fig. 18 these areas are visualized by the corresponding elemental distribution images.

The images also testify to a completely inverse distribution of the elements silicon and boron. Furthermore, carbon and nitrogen are detected in the boron-containing areas, indicating that the phase separation induced by crystallization leads to the segregation of a B–C–N matrix phase at the grain boundaries of the nanocrystals.

An electron energy loss (EEL) spectrum of the matrix phase can be seen in Fig. 19. The presence of boron, carbon and nitrogen is associated with energy losses at 188 eV, 284 eV and 401 eV respectively. The spectrum traces back to area b in between the silicon nitride nanocrystals shown in Fig. 20. In Fig. 21 the atomic ratio B:N:C obtained by the quantitative evaluation of the EEL spectra that trace back to the areas a–c (Fig. 20) is shown. The matrix phase (area b) exhibits an average atomic ratio B:N:C $\approx$ 1:1:3.3. Only close to the Si_3N_4–matrix interface (areas a and c) is a decrease of the ratio C:(B:N) determined.

The results for the composition of the matrix phase are in accordance with the relative phase amounts 17 mol% BN and 27.5 mol% carbon (graphite), which are calculated by the CALPHAD approach up to 1484 °C (Fig. 22) and are equivalent to an atomic ratio B:N:C = 1:1:3.2. Above this temperature the calculated amount of carbon decreases to 13 mol%, connected with the quantitative degradation of the silicon nitride phase combined with an increase of the gas-phase amount (nitrogen) and the phase amount of silicon carbide.

Although the diagram in Fig. 22 does not provide

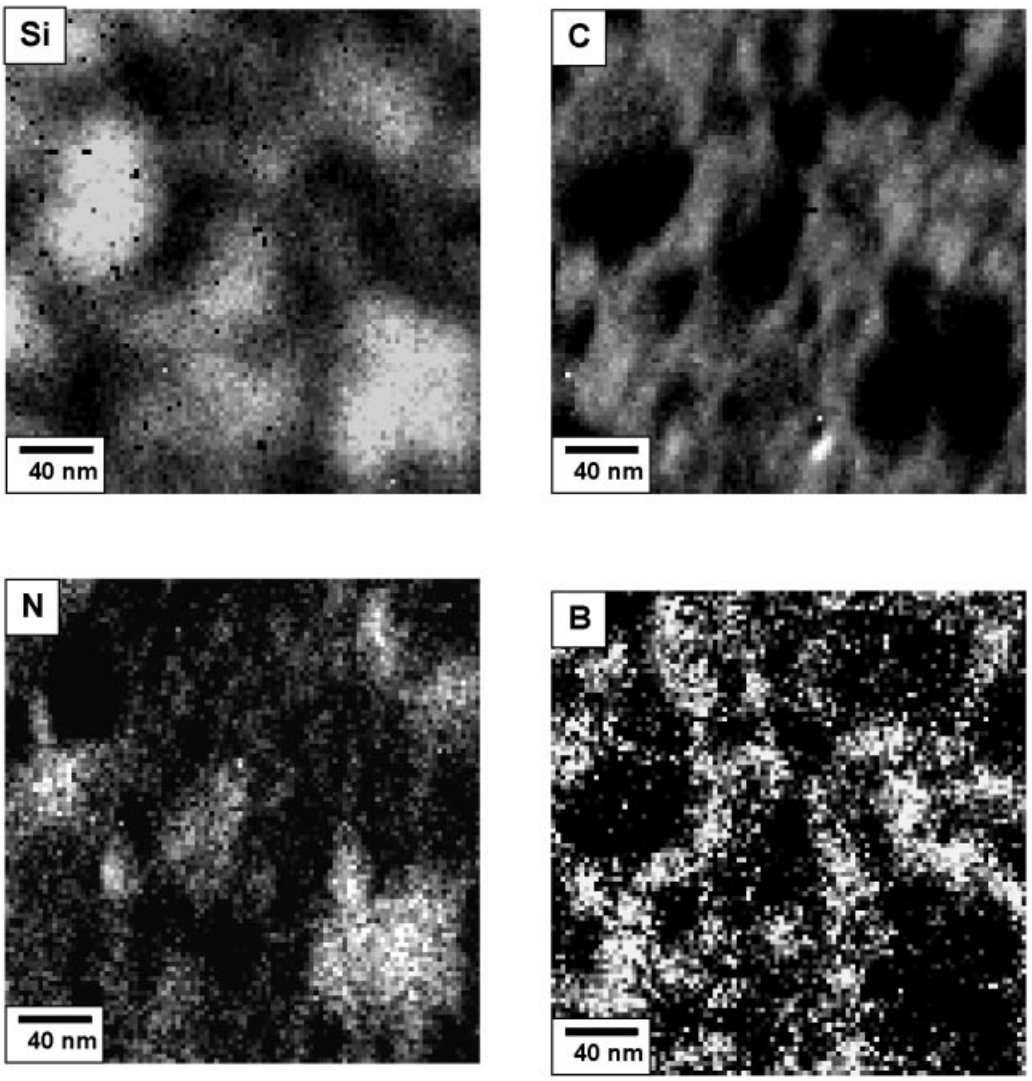

Figure 18 Elemental distribution images of silicon, carbon, nitrogen and boron of the PHBS(p)-derived ceramic after annealing at 1800 °C (5 h, argon).

any description of the turbostratic B–C–N phase, the comparison of the calculated and experimentally determined B:N:C ratio clearly points out that crystallization at 1800 °C initially yields a metastable ceramic solid prior to decomposition by the evolution of nitrogen and the formation of the thermodynamically stable phases. Consequently, no weight loss of the solid phase can be detected after the annealing treatment.

As a result, the phase separation by crystallization leads to the formation of a B–C–N matrix phase with a reduced carbon activity, and thus less reactivity against silicon nitride (according to Eqn [14]), resulting in an increased stability of the embedded silicon nitride. Furthermore, the encapsulation of silicon nitride nanocrystals by the B–C–N matrix phase provides nanocompartments suitable for the stabilization of silicon nitride by an increase of the internal equilibrium nitrogen partial pressure according to Eqn [14]. Owing to the phase equilibria in Fig. 23, a partial pressure of 10 bar shifts the stability of Si_3N_4 in the presence of carbon up to temperatures around 1700 °C.[76,77] Moreover, the same is true with respect to the

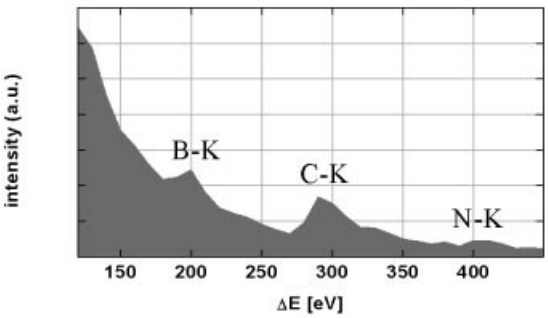

Figure 19 EEL spectrum of B–C–N matrix of area b shown in Fig. 20.

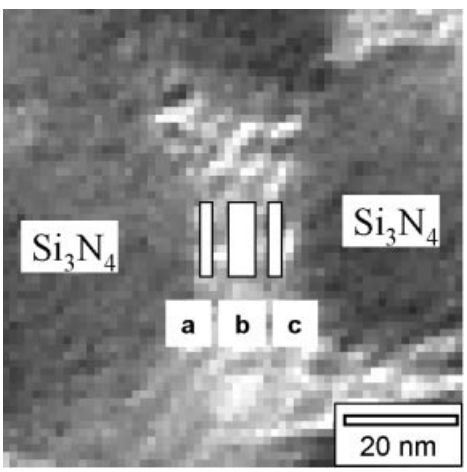

Figure 20 Bright-field image of PHBS(p)-derived ceramic after annealing at 1800 °C (argon, 5 h); areas investigated by EEL spectroscopy are inserted.

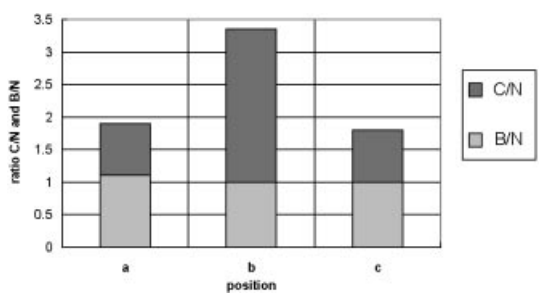

Figure 21 B/N and C/N atomic ratio of areas shown in Fig. 20.

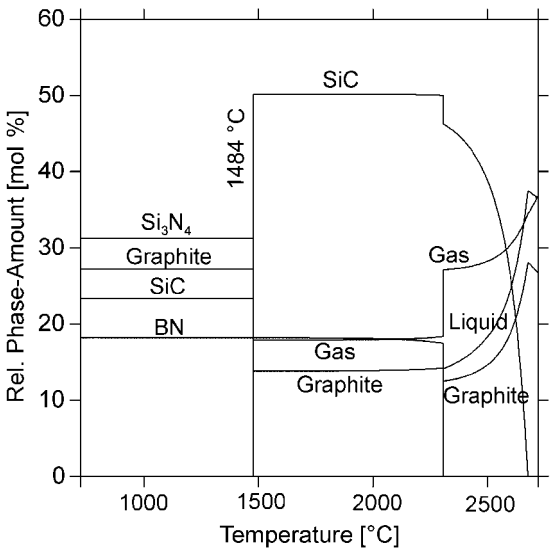

Figure 22 Phase fraction diagram of the PHBS(p)-derived amorphous ceramic (CALPHAD). Phase amounts refer to mole of atoms.

dissociation of silicon nitride into the elements that occurs according to the phase equilibria at 1841 °C (1 bar N_2).[12]

5 CONCLUSIONS

The ceramization of polysilazanes and polysilyl-

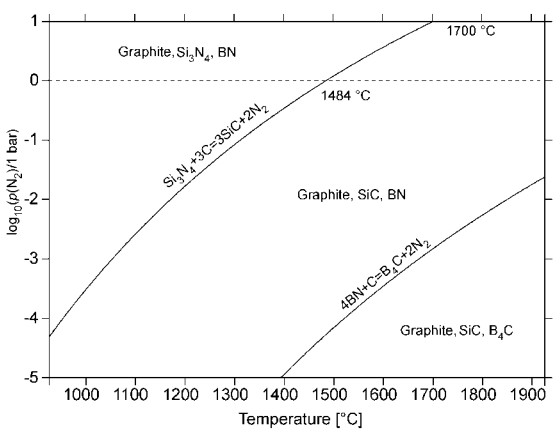

Figure 23 Calculated phase equilibria based on the atomic ratio $Si_{32}C_{56}B_{12}$ valid for the PHBS(p)-derived ceramic solid as a function of the nitrogen partial pressure and temperature (CALPHAD).

carbodiimides considered in this study leads to the formation of ternary amorphous Si–C–N ceramic solids. During the polymer–ceramic conversion, the evolution of Si—N bonds is energetically favored compared with the formation of Si—C bonds, which contributes to the minimization of the Gibbs energy of the system. Finally, silicon nitride segregations with a size in the range between 5 and 10 Å embedded into an amorphous matrix are obtained. The short-range order and the phase formation is influenced strongly by the corresponding phase equilibria. Consequently, the structural units of the thermodynamically stable phases are already preformed within the amorphous ceramic stages.

The phase formation induced by the *in situ* crystallization of the amorphous Si–C–N ceramics is also determined by the thermodynamic equilibria. Depending on the composition of the amorphous ceramic solids, SiC/C as well as Si_3N_4/SiC composites are obtained. Furthermore, this powder-free process leads to the formation of completely clean grain boundaries without any segregation.

The incorporation of boron leads to an increased thermal stability of the amorphous state. As a result of the formation of B—N bonds, the amount of nitrogen available for the formation of Si—N bonds is reduced. Consistent with the results obtained for the ternary system, the short-range order within these amorphous solids is strongly determined by the location of their composition in the Si–B–C–N phase diagram. As a consequence, ceramics that exhibit a composition defined by the four-phase equilibrium $Si_3N_4 + SiC + C + BN$ close to the three-phase equilibrium field $SiC + C + BN$ consist mainly of the structural units of silicon carbide, boron nitride, carbon and silicon carbonitride units SiN_xC_y. Crystallization induces a transformation of these mixed tetrahedra into SiN_4 and SiC_4 units, yielding metastable materials that contain silicon nitride and silicon carbide nanocrystals. Owing to this phase separation, a boron-, carbon- and nitrogen-containing matrix is formed. The silicon nitride crystals are kinetically stabilized by the B–C–N matrix phase, resulting in an extraordinary thermal stability up to 2000 °C.

Acknowledgements The authors thank Professor L. G. Sneddon, University of Pennsylvania, for helpful discussions, as well as for providing the HPZ-derived SiBCN samples for TGA investigations. Furthermore, the financial support of the Deutsche Forschungsgemeinschaft (Priority Program 'Precursor Ceramics' and Graduate Program 'Interfaces in Crystalline Materials') as well as of the Japan Science and Technology Corporation (JST) is gratefully acknowledged.

REFERENCES

1. Lange FF. *J. Am. Ceram. Soc.* 1973; **56**(9): 445.
2. Greil P, Petzow G and Tanaka H. *Ceram. Int.* 1987; **13**: 19.
3. Lange FF. *J. Am. Ceram. Soc.* 1974; **57**(2): 84
4. Rice RW. *Am. Ceram. Soc. Bull.* 1983; **62**: 916
5. Seyferth D and Wiseman GH. *J. Am. Ceram. Soc.* 1984; **67**: C132
6. Peuckert M, Vaahs T and Brück M. *Adv. Mater.* 1990; **2**: 398
7. Bill J and Aldinger F. *Adv. Mater.* 1995; **7**: 775.
8. Baldus HP, Wagner O and Jansen M. *Mater. Res. Soc. Symp. Proc.* 1992; **271**: 821.
9. Laine RM, Babonneau F, Blowhowiak KY, Kennish RA, Rahn JA, Exarhos GJ and Waldner K. *J. Am. Ceram. Soc.* 1995; **78**: 137.
10. Laine RM, Blum YD, Tse D and Glaser R. In *Inorganic and Organometallic Polymers*, *ACS Symposium Series* 360, Zeldin M, Wynne KJ, Allcock HR (eds). American Chemical Society: Washington, DC, 1988; 124.
11. Blum Y and Laine RM. *Organometallics* 1986; **5**: 2081.
12. Seifert HJ, Peng J, Golczewski J and Aldinger F. *Appl. Organomet. Chem.* this issue.
13. Bill J, Schuhmacher J, Müller K, Schempp S, Seitz J, Dürr J, Lamparter HP, Golczewski J, Peng J, Seifert HJ and Aldinger F. *Z. Metallkd.* 2000; **91**: 335.
14. Gerdau T, Kleiner HJ, Peuckert M, Brück M and Aldinger F. *Ger. Offen* DE 37 33 727 A1. 1989.
15. Riedel R, Kleebe HJ, Schönfelder H and Aldinger F. *Nature* 1995; **374**: 526.
16. Bill J and Aldinger F. *Z. Metallkd.* 1996; **87**: 827.
17. Bill J, Seitz J, Thurn G, Dürr J, Canel J, Janos B, Jalowiecki A, Sauter D, Schempp S, Lamparter HP, Mayer J and Aldinger F. *Phys. Status Solidi A* 1998; **166**: 269.
18. Kienzle A, Obermeyer A, Riedel R, Aldinger F and Simon A. *Chem. Ber.* 1993; **126**: 2569.
19. Obermeyer A, Kienzle A, Weidlein J, Riedel R and Simon A. *Z. Anorg. Allg. Chem.* 1994; **620**: 1357.
20. Kienzle A, Bill J, Aldinger F and Riedel R. *Nanostruct. Mater.* 1995; **6**: 349.
21. Schuhmacher J, Weinmann M, Bill J, Aldinger F and Müller K. *Chem. Mater.* 1998; **10**(12): 3913.
22. Seyferth D, Strohmann C, Dando NR, Perrotta AJ and Gardner JP. *Mater. Res. Soc. Symp. Proc.* 1994; **327**: 191.
23. Bill J, Aldinger F, Kienzle A and Riedel R. *Ger. Offen*. DE 44 30 817 A1, 1996.
24. Gabriel AO, Riedel R, Storck S and Maier WF. *Appl. Organomet. Chem.* 1997; **11**: 833.
25. Huggins J. *Ger. Offen*. DE 411 42 17 A1, 1992.
26. Polyhydridomethylsilazane (PHMS), product information NCP 200. Nichimen Corp.: Tokyo, Japan.
27. Takamizawa M, Kobayashi T, Hayashida A and Takeda Y. *US Patent* 4 550 151, 1985.

28. Takamizawa M, Kobayashi T, Hayashida A and Takeda Y. *US Patent* 4 604 367, 1986.
29. Seyferth D and Plenio H. *J. Am. Ceram. Soc.* 1990; **73**: 2131.
30. Seyferth D, Plenio H, Rees Jr WS and Bücher K. In *Frontiers of Organosilicon Chemistry, Proceedings of IXth International Symposium on Organosilicon Chemistry*, Bassindale AR, Gaspar PP (eds). Royal Society of Chemistry: Cambridge, UK, 1991.
31. Interrante LV, Hurley Jr WJ, Schmidt WR, Kwon D, Doremus RH, Marchetti PS and Maciel GE. *Ceram. Trans. (Adv. Compos. Mater.)* 1991; **19**: 3.
32. Funayama O, Arai M, Aoki H, Tashiro Y, Katahata T, Sato K, Isoda T, Suzuki T and Kohshi I. *US Patent* 5 128 286, 1992.
33. Srivastava D, Duesler EN and Paine RT. *Eur. J. Inorg. Chem.* 1988; 855.
34. Su K, Remsen EE, Zank GA and Sneddon LG. *Chem. Mater.* 1993; **5**: 547.
35. Su K, Remsen EE, Zank GA and Sneddon LG. *Polym. Prepr.* 1993; **34**: 334.
36. Wideman T, Fazen PJ, Su K, Remsen EE, Zank GA and Sneddon LG. *Appl. Organomet. Chem.* 1998; **12**: 1.
37. Jansen M and Baldus HP. *Ger. Offen*. DE 410 71 08 A1, 1992.
38. Baldus HP, Wagner O and Jansen M. *Mater. Res. Soc. Symp. Proc.* 1992; **271**: 821.
39. Baldus HP and Jansen M. *Angew. Chem.* 1997; **109**: 338. *Angew. Chem. Int. Ed. Engl.* 1997; **36**: 328.
40. Jüngermann H and Jansen M. *Mater. Res. Innovat.* 1999; **2**: 200.
41. Jones PR and Myers JK. *J. Organomet. Chem.* 1972; **34**: C9.
42. Ruwisch LM, Dressler W, Reichert S and Riedel R. In *Organosilicon Chemistry III, From Molecules to Materials*, Auner N, Weis J (eds). Wiley–VCH: Weinheim, 1997; 628.
43. Ruwisch LM. Riedel R. *Electrochem. Soc. Proc.* 1997; **97-39**: 355.
44. Ruwisch LM. *PhD Thesis*, Technische Universität Darmstadt, 1998.
45. Riedel R, Ruwisch LM, An L and Raj R. *J. Am. Ceram. Soc.* 1998; **81**: 3341.
46. Riedel R, Kienzle A, Petzow G, Brück M and Vaahs T. *Ger. Offen*. DE 432 07 83 A1, 1994.
47. Riedel R, Kienzle A, Petzow G, Brück M and Vaahs T. *Ger. Offen*. DE 432 07 84 A1, 1994.
48. Bill J, Kienzle A, Sasaki M, Riedel R and Aldinger F. In *Ceramics: Charting the Future*, Vincenzini P (ed.). Techna Sri: 1995.
49. Riedel R, Kienzle A, Dressler W, Ruwisch LM, Bill J and Aldinger F. *Nature* 1996; **382**: 796.
50. Choong Kwet Yive NS, Corriu RJ, Leclercq D, Mutin PH and Vioux A. *New J. Chem.* 1991; **15**: 85.
51. Weinmann M, Schuhmacher J, Kummer H, Prinz S, Peng J, Seifert HJ, Christ M, Müller K, Bill J and Aldinger F. *Chem. Mater.* in press.
52. Bill J and Aldinger F. Precursor-derived covalent ceramics. In *Precursor-Derived Ceramics*, Bill J, Wakai F, Aldinger F (eds). Wiley–VCH: 1999; 33.
53. Weinmann M and Aldinger F. Temperature stable ceramics from inorganic polymers. In *Precursor-Derived Ceramics*, Bill J, Wakai F, Aldinger F (eds). Wiley–VCH: 1999; 83.
54. Matsumoto RLK and Schwark JM. Eur. Patent 0 536 698 A1, 1993.
55. Bill J, Aldinger F and Kienzle A and Riedel R. German Patent DE 44 47 534 C2, 1994.
56. Bill J and Aldinger F. *Z. Metallkd.* 1996; **87**: 827.
57. Weinmann M, Haug R, Bill J and De Guire M and Aldinger F. *Appl. Organomet. Chem.* 1998; **12**: 725.
58. Weinmann M, Haug R, Bill J, Aldinger F, Schuhmacher J and Müller K. *J. Organomet. Chem.* 1997; **541**: 345.
59. Weinmann M, Kamphowe TW, Fischer P and Aldinger F. *J. Organomet. Chem.* 1999; **592**: 115.
60. Kamphowe TW, Weinmann M, Bill J and Aldinger F. *Silic. Ind.* 1998; **63**: 159.
61. Kamphowe TW. *PhD Thesis*, Universität Stuttgart, 1999.
62. Weinmann M, Kamphowe TW, Schuhmacher J, Müller K and Aldinger F. *Chem. Mater.* submitted for publication.
63. Burns GT, Angelotti TP, Hannemann LF, Chandra G and Moore JA. *J. Mater Sci.* 1987; **22**: 2609.
64. Choong Kwet Yive NS, Corriu RJ, Leclercq D, Mutin PH and Vioux A. *Chem. Mater.* 1992; **4**: 1263.
65. Blum YD, Schwartz KB and Laine RM. *J. Mater. Sci.* 1989; **24**: 1707.
66. Sugimoto M, Shimoo T, Okamura K and Seguchi T. *J. Am. Ceram. Soc.* 1995; **78**(4): 1013.
67. Sugimoto M, Shimoo T, Okamura K and Seguchi T. *J. Am. Ceram. Soc.* 1995; **78**(7): 1849.
68. Dürr J, Schempp S, Lamparter HP, Bill J, Steeb S and Aldinger F. *Solid State Ionics* 1997; **101–103**: 1041.
69. Bill J, Frieß M, Aldinger F and Riedel R. *Proc. Mater. Res. Symp. Proc.* 1994; **346**: 605.
70. Seifert HJ and Aldinger F. in Symp. on Int. Joint Ceramics Superplasticity: New Properties from Atomic Level Processing, Japan Science and Technology Corporation, Tokyo, Japan, Nov 10–11 1999, 8–15.
71. Jalowiecki A, Bill J, Aldinger F and Mayer J. *Composites Part A* 1996; **27A**: 717.
72. Schuhmacher J, Müller K, Weinmann M, Bill J and Aldinger F. Proc. Werkstoffwoche 98, Symposium 9b: Physik und Chemie der Keramik, 12–15 October, 1998, Munich (in German).
73. Schuhmacher J, Berger F, Weinmann M, Bill J, Aldinger F and Müller K. *Appl. Organomet. Chem.* this issue.
74. Schuhmacher J. *PhD Thesis*, Universität Stuttgart, 2000
75. Müller K. In *Precursor-Derived Ceramics*, Bill J, Wakai F, Aldinger F (eds). Wiley–VCH: 1999; 197.
76. Seifert HJ, Lukas HL and Aldinger F. *Ber. Bunsenges. Phys. Chem.* 1998; **9**: 1309.
77. Seifert HJ and Aldinger F. In *Precursor-Derived Ceramics*, Bill J, Wakai F, Aldinger F (eds). Wiley–VCH: 1999; 165.

